



Seismic Isolators Layout Optimization Using Genetic Algorithm Within the Pymoo Framework

Adil El Ouardani ^{1*} , Taoufik Tbatou ¹

¹ Faculty of Sciences and Techniques FST, LSIB Laboratory, Hassan II University of Casablanca, Mohammedia, Morocco.

Received 22 April 2024; Revised 03 July 2024; Accepted 09 July 2024; Published 01 August 2024

Abstract

In most previous studies, seismic base isolation system optimization has mainly focused on determining isolation layer parameters. However, the subsequent steps of isolator device selection and positioning can significantly impact overall system performance. To address these shortcomings, we propose an alternative optimization approach demonstrated through two models: regular and irregular 8-storey reinforced concrete structures. This approach utilizes the Pymoo framework and commercially available isolators to find optimal isolator layout configurations in two steps. First, using the equivalent lateral force (ELF) procedure, an initial population of seismic isolators meeting shear strain, base shear coefficient, and buckling requirements was randomly selected from suppliers' elastomeric bearing catalogs. Second, the Non-dominated Sorting Genetic Algorithm II (NSGA-II) was used to improve the seismic response of the models under the fast nonlinear analysis (FNA) method by minimizing peak roof acceleration, inter-story drift ratio, displacement of the isolated base layer, as well as maximizing the fundamental period. The results underscore the effectiveness of this approach in improving seismic response. Compared to fixed-base structures, the optimal solutions achieved more than double the fundamental period, reduced peak roof acceleration by over 70%, and diminished base shear force by approximately 50%. This methodology can serve as a reference for future research across various structure types, including hybrid isolation systems and steel structures.

Keywords: Seismic Isolation; Metaheuristic Algorithms; Rubber Bearings; Multi Objective Optimization; Pymoo.

1. Introduction

1.1. Design Of Isolation System

Today, seismic base isolation technology is a justified, mature, and extremely effective way for protecting structures and their contents from earthquake damage. In contrast to the traditional seismic approach, which aims to provide structures with adequate strength, stiffness, and ductility, this approach remains highly effective and recommended, especially for large and important structures such as hospitals, storage tanks, and fire stations, etc., because they contain valuable equipments and must remain operational during and after an earthquake [1].

Seismic isolation aims to decouple the structure from the horizontal components of ground motion. This is accomplished by installing an isolation system comprising isolators and dampers between the building and its foundation, and in some cases, at different levels of the structure. This system has a low horizontal stiffness but a high vertical stiffness, which increases the fundamental period of the building significantly compared to its fixed base period [2]. Most seismic isolation techniques use elastomer bearings and sliding bearings, combined with or without vibration

* Corresponding author: adil.elouardani-etu@etu.univh2c.ma

 <http://dx.doi.org/10.28991/CEJ-2024-010-08-07>



© 2024 by the authors. Licensee C.E.J, Tehran, Iran. This article is an open access article distributed under the terms and conditions of the Creative Commons Attribution (CC-BY) license (<http://creativecommons.org/licenses/by/4.0/>).

control devices (lead dampers, oil dampers, etc.). Rubber-based isolators are particularly prevalent in Japan [3]. These rubber isolators can be divided into three main types:

- Natural rubber bearings, which generally have a linear behavior (Figure 1);

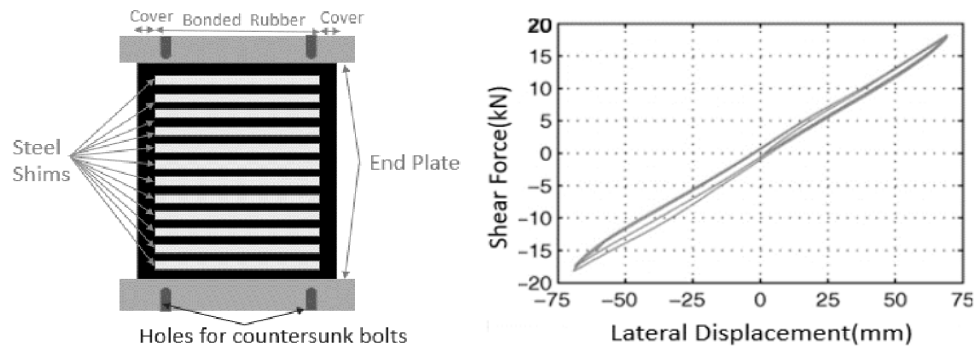


Figure 1. A schematic view and linear behavior of NRB [1]

- Lead rubber bearings [4-6], generally modeled by bilinear behavior characterized by a set of parameters such as effective stiffness (K_{eff}), equivalent damping (C_{eff}), characteristic strength (Q_d), and post-yield stiffness (K_d) (Figure 2).

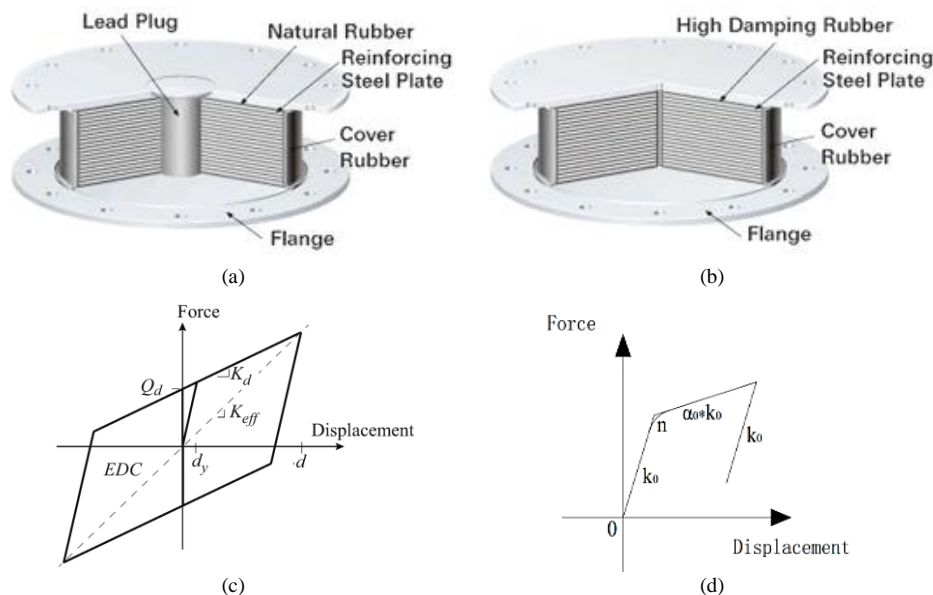


Figure 2. (a) Lead Rubber Bearing, (b) High Damping Rubber Bearing [7], (c) Bilinear behavior [3], (d) Bouc wen model [8]

- High damping rubber bearing, commonly modeled by the Bouc-Wen model represented by a combination of a linear spring and a hysteretic spring [8-10].and in some studies the DHI model has also been used [11, 12].

Several methods have been proposed for designing seismic isolation systems. One such method is the Point of Performance Method (PPM) for the design of lead rubber bearing (LRB) isolators, proposed by Kazeminezhad et al. [13]. This method seeks to identify a point of intersection between the capacity (represented by bilinear behavior) and demand (represented by the force-displacement spectrum) curves. Another approach aligning with the latest version of the EC8 code and including stability checks was developed by Losanno et al. [14] for high damping rubber bearing (HDRB) isolators. Ye et al. [15] have proposed a design procedure based on direct displacement of the seismic isolation system with lead rubber bearings. The aim is to achieve performance targets set by displacement thresholds. Numerous studies have been carried out on the design of seismic isolation, defining target values such as the period and damping of the first mode of the isolated building. Typically, these values are 2 to 3 seconds for the period and 20 to 35% for the damping [16-18].

The Equivalent Lateral Force (ELF) procedure, which employs effective stiffness and effective damping, is also used as a simplified analysis method for isolated structures. This method is proposed in seismic codes. It reduces the calculation effort, simplifies the design procedure and serves as a verification tool for non-linear time history analysis [1]. A simplified method has been developed by Keikha & Amiri [19] combining the equivalent lateral force procedure with the capacity spectrum method. This method is evaluated on the basis of maximum isolator displacements and base shears for isolated structures that are equipped with recently invented quintuple friction pendulum isolators.

1.2. Optimization of Seismic Isolation and Vibration Control Systems

Recently, various metaheuristic optimization techniques have been employed to search for optimal parameters in isolation systems. Pourzeynali & Zarif [20] utilized NSGA II to determine the optimal parameters for isolators, aiming to simultaneously minimize the displacement of the building's top floor and the base isolation system. However, this method involves numerous iterative calculations and does not consider the 3D model. Bakhshinezhad & Mohebbi [21] also used the same algorithm to find an optimal design for semi-active fluid viscous dampers. However, this study is limited to an eight-story nonlinear shear building frame with hysteretic bilinear elastoplastic behavior. Tsipianitis & Tsompanakis [22] employed a swarm intelligence algorithm to optimize the size of key parameters for SFPB and TFPB isolators in a base-isolated storage tank. They aimed to minimize accelerations transmitted to the superstructure while adhering to damping and vibration period constraints. In another study, Tsipianitis et al. [23] used a cuckoo search (CS) to optimize key design parameters and the placement of minimum-friction isolators at the base of the tank to minimize the eccentricity between the center of mass and the center of stiffness of the isolation system. However, seismic fragility was checked separately for optimal solutions and was not included in the optimization problem. Zou and Yan [24] used a convolutional neural network and a Hunter-prey optimization algorithm to improve the optimal dimensions and arrangements of bearings. However, the optimized isolation scheme is limited by predefined bearing sizes. Babaei et al. [25] turned to NSGA II and fuzzy logic to enhance the optimal design of MR Dampers.

Çerçevik et al. [26] conducted a study that used three bio-inspired search methods (crow search, whale optimization, and grey wolf optimizer) to determine the optimal isolation parameters of a shear frame model with base isolation under seismic excitations. Pal et al. [27] used a genetic algorithm, implemented in a C++ program, to optimize the base isolation parameters of a concrete frame structure. A two-stage isolator optimization study was conducted by Dang et al. [28] using a genetic algorithm and an integer programming method. However, in the second stage, the isolator layout was constrained by a limited isolator size, and there might still be a slight difference between the optimal isolator layer parameters obtained in the first stage and those corresponding to the optimal configuration retained in the second optimization stage. In one study, Fallah & Zamiri [29] used the NASG-II algorithm to find the optimum parameters of a sliding-bearing isolation system for a shear-type structure. This system aims to simultaneously minimize the displacement and acceleration of the upper floor of the building, along with the displacement at the base. In another study, Fallah & Honarparast [30] optimized the location of Pall friction dampers to satisfy the desired objective functions. Song et al. [31] proposed a two-stage optimization approach to enhance the seismic resilience of hospitals. The first step optimizes the design of the isolation layer to minimize displacement and functional losses. The second stage focuses on improving non-structural components and medical equipment, using NSGA II, Bayesian networks, and discrete-event simulation to assess room availability and treatment capacity for earthquake victims.

The parameters of the seismic isolation system in a shear structure are optimized by Kandemir and Mortazavi [32] using the fuzzy differential evolution method incorporating a virtual mutant (FDEV). This optimization involves minimizing the ratio between the peak roof acceleration (PRA) and the peak ground acceleration (PGA) while considering limits imposed on the maximum displacement, damping ratios, and the period of the isolation system. Ocak et al. [33] used an adaptive harmony search algorithm to optimize the isolator period and damping ratio to minimize the maximum acceleration while taking into account three distinct limits of damping ratio and isolator displacement. Taymus et al. [34] used metaheuristic algorithms such as artificial bee colonies, crow search, and Archimedes' method to optimize the weight of steel frames isolated by triple-friction pendulums, taking into account inter-story drift, roof displacement, and structural constraints. A comparative study of metaheuristic algorithms carried out by Öncü-Davas et al. [35], aimed at minimizing the peak roof-to-ground acceleration ratio of nonlinear seismic isolation systems during near-fault earthquakes, taking into account the flexibility of the superstructure, showed that the GWO, JA, and TLBO algorithms are effective in solving such optimization problems. In their study, Ocak et al. [36] explored the use of metaheuristic algorithms such as floral pollination algorithm (FPA), harmony search (HS), teaching learning-based optimization (TLBO), and Jaya algorithms (JA) to optimize the period and damping ratio of low, medium, and high damping base isolators. The objective was to minimize the displacement and total acceleration of the structure, taking into account soil-structure interaction on three different soil types.

In addition, the configuration of the isolation layer in the current optimization process is often restricted to a predefined set of sizes and a fixed distribution of isolation devices, based on experience or test results, without exploring other possible configurations. Previous studies, as summarized in Table 1, focus on optimizing the parameters of the isolation layer corresponding to target values as constraints (such as target period and damping). The goal is to improve the structure's response by minimizing, for example, peak roof acceleration, inter-story drift ratio, and displacements. However, a major difficulty arises once the optimal parameters of the isolation layer are obtained, which is selecting and arranging seismic isolators and/or dampers requires finding a compromise between ideal design properties and those available in manufacturers' catalogs.

The geometry of the isolator resulting from optimization procedures may not correspond to what is available on the market because this necessitates project-specific manufacturing or dimensional adjustments that could slightly

compromise the optimization of the isolated structure. Therefore, several aspects should be considered or improved at the end of previous research works:

- Explore multiple isolator arrangement configurations.
- Use Multiple sizes and types of isolators within the same isolation layer.
- Take into account real data on isolators from suppliers' catalogs.

Table 1. Main studies employing metaheuristic search methods in the field of seismic isolation and vibration control

Ref.	Aim of the Study	Characteristics of the Optimization Problem		
		Design Variables	Objectives Functions & Constraints	Search Methods
[20]	Search for optimal values of isolator bearing parameters that minimize the horizontal displacement of the building's top story and base isolation layer	Mass, Stiffness, and Damping ratio	Horizontal displacement at the top story Horizontal displacement of base isolation layer	NSGA-II Algorithm
[21]	Optimal design of semi-active fluid viscous dampers by minimizing the Mean inter-story drift and absolute acceleration	Maximum Damping coefficient and Weighting matrices	Mean inter-story drift The mean of absolute acceleration	NSGA-II Algorithm
[22]	Optimizing the sizing of the main parameters of the SFPB and TFPB isolators to improve the seismic response of liquid storage tanks isolated from the base	The friction coefficient and the radius of curvature of the sliding surfaces	Transmitted accelerations to the superstructure subject to Damping ratio and period limitation	Cuckoo search, Particle swarm optimizer, hybrid CS-BSA and ECS (enhanced cuckoo search)
[23]	Optimizing the critical design parameters and the placement of the minimum number of isolators at the base of the tank	The friction coefficient and the radius of curvature of the sliding surfaces	Minimizing the eccentricity of the isolation system subject to the damping ratio and period limitation	Cuckoo search optimizer
[24]	Predict and optimize the layout of isolation bearings	Type and placement of isolator bearings	The seismic decrease coefficient, story drift ratio, and total cost of bearings are subject to the damping ratio and period limitation.	Convolutional Neural Network & Hunter-prey optimization algorithm
[25]	The optimal position of MR Dampers to control and reduce the structure's response under earthquakes	Placement of MR Dampers	Maximum displacement, acceleration, and inter-story drift of the top floor	NSGA-II & fuzzy logic
[26]	Obtaining and comparing optimum isolation parameters by minimizing the desired objectives functions by applying three bio-inspired search methods	Periods and effective damping ratio	Peak Roof Acceleration to Peak Ground Acceleration ratio subject to base isolation displacement limit	Crow search (CSA), Whale optimization (WOA) and grey wolf optimizer (GWO)
[27]	Optimizing the base isolation parameters of concrete frame structure that leads to reducing the PRA (peak roof acceleration) based on soil conditions	Damping and Stiffness	Peak Roof Acceleration ratio subject to Period limitation and soil condition	Genetic algorithm GA
[28]	Optimization of the Bearing Layout of Isolated Structure	Equivalent stiffness, Yield and ultimate displacement	Earthquake reduction coefficient, Bearing displacement, inter-story drift and cost of bearings	Multi population genetic algorithm (MPGA) & integer programming
[29]	Finding the optimal values of isolator parameters of the restoring force device.	Friction coefficient, Mass and Damping ratios	Building's top story displacement and acceleration, and the base raft's displacement	NSGA-II Algorithm
[30]	Optimizing the placement of Pall friction dampers to satisfy the desired objective functions	The slip load value	Peak displacements, Peak accelerations of top roof and Peak base shear ratios before and after dampers installation	NSGA-II Algorithm
[32]	Determining the optimal values of the parameters of a seismic isolation system of the base-isolated building by minimizing desired objectives functions	Stiffness and damping coefficient	Peak roof acceleration (PRA) to the peak ground acceleration (PGA) ratio subject to maximum displacement limitation, damping ratios range, and period range	fuzzy differential evolution method incorporating a virtual mutant (FDEVM)
[33]	The optimization of the period and damping ratio of an isolator placed on the base of a (SDOF) structure to reduce the acceleration.	Period and damping ratio	The maximum acceleration subject to the limit of displacement of the isolation system and different damping ratio	Adaptive harmony search algorithm (AHS)

To address these gaps, we propose an alternative two-step optimization approach. This method utilizes catalogs and devices available on the market to directly find optimal arrangements of isolation systems from suppliers' catalogs, aiming to enhance the seismic response of isolated structures.

2. Material and Methods

2.1. Initial Population Generation

After generating the initial population using the ELF procedure, a non-dominated elitist algorithm (NSGA-II) was used to find optimal arrangements of isolation devices that improved the seismic response under the fast non-linear time history analysis (FNA) by minimizing the peak roof acceleration, the isolator displacements, and the inter-story drifts, as well as maximizing the fundamental period of the isolated structure. To achieve this, we used ETABS OAPI to interact with the ETABS V21 software and Python programming interface, taking advantage of the Pymoo framework developed by Blank & Deb [37], which comprises a set of Python modules and packages for solving simple, multi-objective, and many-objective optimization problems. In the proposed method, the isolation layer is optimized by considering a different approach to those commonly adopted and described above, starting with suppliers' catalogs and the isolation

devices available on the market, to build the optimization procedure in two steps. The first step aims to generate the initial population from commercially available catalogs, satisfying design targets through the application of the Equivalent Lateral Force (ELF) method, while the second step focuses on optimizing the arrangement of isolators, leading to improved seismic performance of the base-isolated structure.

Based on the axial column load (DL+0.3LL) and the ELF approach as shown in Figure 3, the initial population is generated by randomly selecting a set of isolators from the three series (HH, LH, NH) in the Bridgestone Corporation catalog [12], meeting the specified below criteria, which are derived from the study conducted by Murota et al. [38].

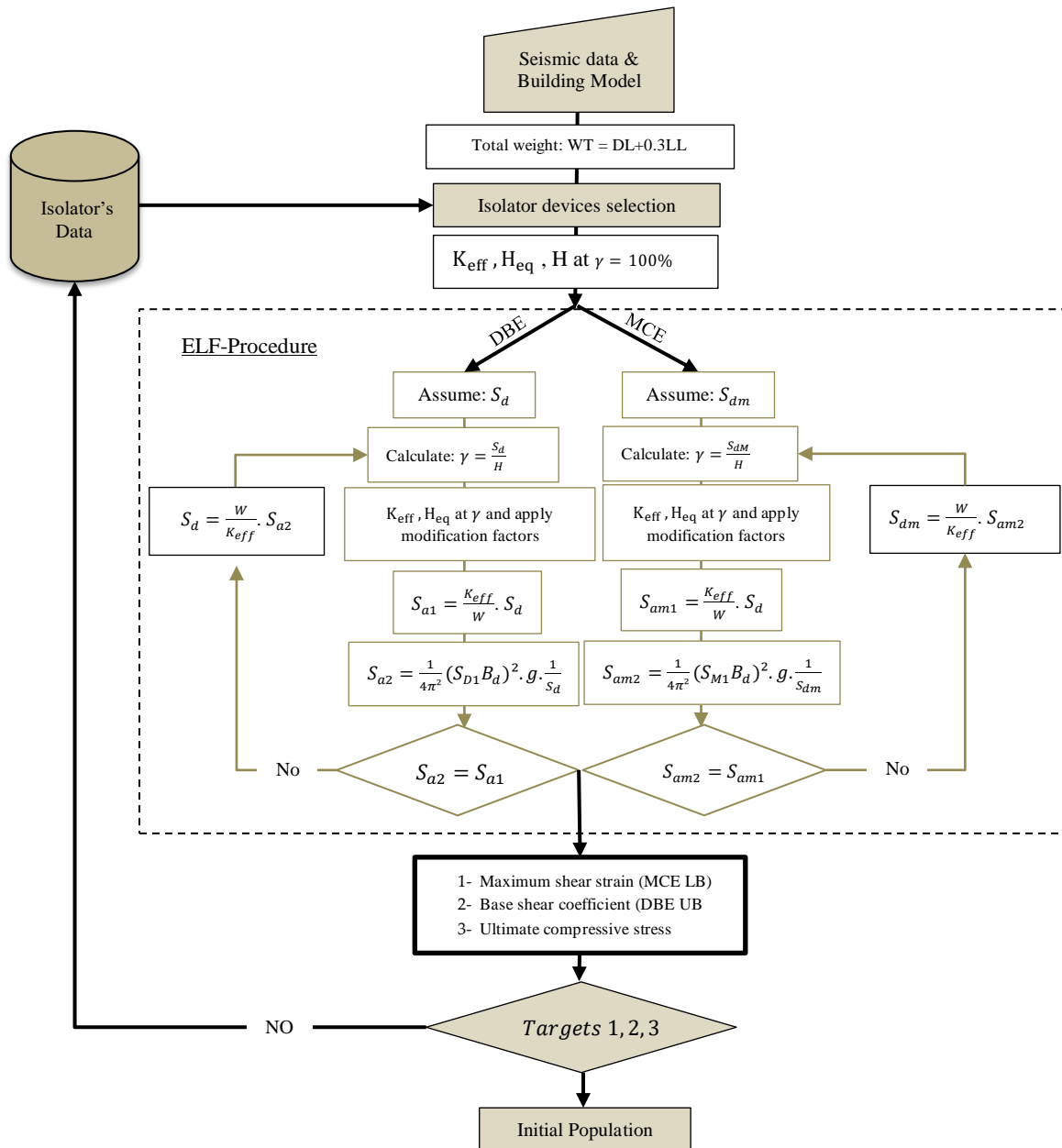


Figure 3. Initial population generation flow chart using ELF approach

All bearing specifications, and the dependence of the mechanical properties of isolators, particularly for the upper and lower limits, such as damping ratio (H_{eq}), effective stiffness (K_{eff}), post-yield stiffness (K_d), and characteristic strength (Q), on aging, temperature, manufacture, and test conditions are shown in Table 2 and available in the product catalog.

- **Target 1:** Maximum shear strain considering torsion effect shouldn't exceed the allowable value under lower bound: $\gamma_{max} \leq 270\%$ in MCE case.
- **Target 2:** Maximum base shear coefficient should be under 20%: $\frac{V_b}{W} \leq 0.2$ in DBE case with upper bound.
- **Target 3:** Ensuring stabilities against buckling and shear strain for each device under static load (DL+0.3LL) for maximum considering earthquake (MCE).

Table 2. Properties modification factors for the selected devices

Property Modification Type	HDRB /X0.4S				LRB/G4				NRB/G4	
	K _{eff}		H _{eq}		K _d		Q _d		K _{eff}	
	UB	LB	UB	LB	UB	LB	UB	LB	UB	LB
Manufacturing variation λ _{spec}	1.1	0.9	0.9	1.1	1.1	0.9	1.1	0.9	1.1	0.9
Aging λ _a	1.1	1	0.9	1	1.1	1	1	1	1.1	1
Temperature: λ _t	1.21	0.84	1.07	0.88	1.06	0.95	1.23	0.79	1.06	0.95
Total λ	1.41	0.74	0.87	0.98	1.26	0.85	1.33	0.69	1.26	0.85

The design variables correspond to the layout of the isolators and can be represented by the design vector $X = [x_1 \ x_2 \ \dots \ x_m]$. While $x_{1 \leq i \leq n}$ represents the number of isolators. In this study, each set of isolators consists of 10 units, as shown in Table 3. This table summarizes information on these isolation devices, including trade names, and mechanical properties of the seismic isolators under a shear strain of 100 %, such as damping ratio, initial stiffness, post-yield stiffness, strength characteristics, as well as geometric dimensions. The design vector (list of isolators) is randomly selected from product catalogs and then the ELF procedure, which is expressed below, is applied. The dimension of this vector corresponds to the number of variables, determined by placing the same isolators under columns transmitting similar or close loads to the foundation. An illustrative example is given in Table 4 to clarify this point.

$$S_a = \frac{S_{D1}}{T} B_d \tag{1}$$

$$B_d = \left(\frac{0.1}{0.05 + H_{eq}} \right)^{0.5} \tag{2}$$

$$S_a g = \left(\frac{2\pi}{T} \right)^2 S_d \tag{3}$$

where S_a is the spectral response acceleration of isolated structure with g unit (9.806 m/s^2), S_{D1} is $S_a(T = 1\text{s})$ for 5% damping ratio is the design spectral response acceleration, B_d is reduction factor of response acceleration, S_d is Spectral response displacement.

S_a can be expressed by:

$$S_a = \frac{1}{4\pi^2} (S_{D1} B_d)^2 \cdot g \cdot \frac{1}{S_d} \tag{4}$$

$$S_a = \frac{K_{eff}}{W} \cdot S_d \tag{5}$$

$$K_{eff} = \sum_{i=1}^m n_i K_{eff,i} \tag{6}$$

$$H_{eq} = \frac{\sum_{i=1}^m n_i K_{eff,i} \cdot H_{eq,i}}{\sum_{i=1}^m n_i K_{eff,i}} \tag{7}$$

where, m is number of isolator types, $K_{eff,i}$, $H_{eq,i}$, n_i are the equivalent stiffness, damping ratio, and the number of the i^{th} isolator.

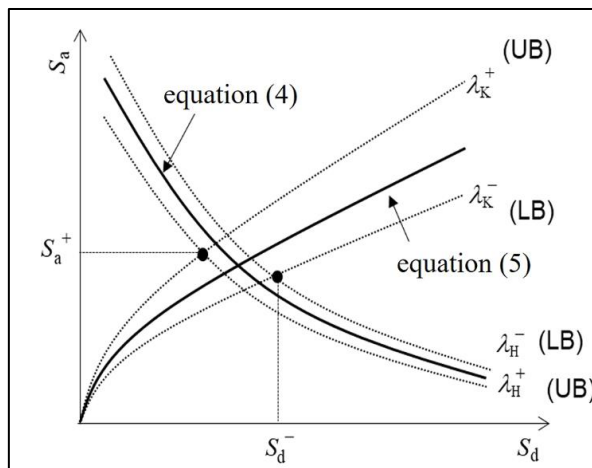
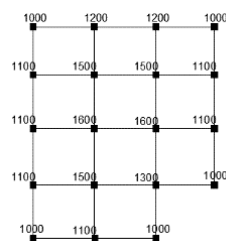


Figure 4. Relationship of Equations 4 and 5, and solution in Sa-Sd plot [38]

Table 3. Properties of seismic isolators at 100% shear strain used in this study

Serie	No	Name	Equivalent shear stiffness K_{eff} (KN/m)	Equivalent Damping ratio H_{eq}	Initial stiffness K_1 (KN/m)	Strength Characteristic Q_d (KN)	Post Yield ratio	Yield Force F_y (KN)	Compressive stiffness (KN/m)	Outer diameter (mm)	Lead plug diameter (mm)	First Shape Factor	Second Shape Factor	Weight W (KN)	Damping C (KN. S/m)*
NH Serie (H=20cm)	1	NH060G4	554	0	-	-	-	-	137000	600	--	36.6	3	6.5	0
	2	NH065G4	657	0	-	-	-	-	1610000	650	--	36.1	3.28	7	0
	3	NH070G4	746	0	-	-	-	-	1840000	700	--	36.4	3.46	7.9	0
	4	NH075G4	866	0	-	-	-	-	2140000	750	--	36.8	3.75	8.9	0
	5	NH080G4	986	0	-	-	-	-	2420000	800	--	36.1	4	11.9	0
	6	NH085G4	1110	0	-	-	-	-	2750000	850	--	36.4	4.26	12.9	0
	7	NH090G4	1260	0	-	-	-	-	3110000	900	--	36.7	4.55	14.6	0
	8	NH095G4	1400	0	-	-	-	-	3450000	950	--	36.3	4.79	15.6	0
	9	NH100G4	1530	0	-	-	-	-	3770000	1000	--	36.4	4.98	17.3	0
	10	NH110G4	1860	0	-	-	-	-	4530000	1100	--	35.3	5.51	20.1	0
LH Serie (H=20 cm)	11	LH060G4-10	865	0.219	7180	62.6	0.0768	62.600	1670000	600	100	37.5	3	6.7	10.646
	12	LH060G4-11	932	0.244	7200	75.7	0.0769	75.700	1670000	600	110	37.5	3	6.7	12.312
	13	LH065G4-10	969	0.199	8490	62.6	0.077	62.600	1970000	650	100	36.9	3.28	7.2	10.614
	14	LH070G4-10	1050	0.181	9630	62.5	0.0769	62.500	2250000	700	100	37.2	3.46	8.1	10.659
	15	LH070G4-11	1120	0.205	9650	75.7	0.0768	75.700	2250000	700	110	37.2	3.46	8.1	12.468
	16	LH075G4-10	1240	0.187	11200	75.7	0.0767	75.700	2610000	750	110	37.5	3.75	9.1	12.684
	17	LH075G4-12	1310	0.209	11200	90.1	0.0769	90.100	2610000	750	120	37.5	3.75	9.2	14.651
	18	LH080G4-12	1430	0.193	12700	90.1	0.0771	90.100	2960000	800	120	37	4	12.2	16.278
	19	LH080G4-14	1600	0.232	12800	123	0.0768	123.000	2960000	800	140	37	4	12.3	20.782
	20	LH085G4-14	1730	0.216	14400	123	0.077	123.000	3360000	850	140	37.3	4.26	13.3	20.922
HH Serie (H=20cm)	21	HH060X4S	554	0.24	3280	45.2	0.1	45.2	1700000	600	--	36.6	3	6.5	9.196
	22	HH065X4S	657	0.24	3890	53	0.1	53	2020000	650	--	36.1	3.28	7	10.393
	23	HH070X4S	746	0.24	4420	61.5	0.1	61.5	2290000	700	--	36.4	3.46	7.9	11.765
	24	HH075X4S	866	0.24	5120	70.6	0.1	70.6	2660000	750	--	36.8	3.75	8.9	13.454
	25	HH080X4S	986	0.24	5830	80.3	0.1	80.3	3030000	800	--	36.1	4	11.9	16.6
	26	HH085X4S	1110	0.24	6600	90.7	0.1	90.7	3420000	850	--	36.4	4.26	12.9	18.338
	27	HH090X4S	1260	0.24	7450	102	0.1	102	3870000	900	--	36.7	4.55	14.6	20.786
	28	HH095X4S	1400	0.24	8290	113	0.1	113	4300000	950	--	36.3	4.79	15.6	22.648
	29	HH100X4S	1530	0.24	9060	126	0.1	126	4700000	1000	--	36.4	4.98	17.3	24.933
	30	HH110X4S	1860	0.24	11000	152	0.1	152	5690000	1100	--	35.3	5.51	20.1	29.632

Table 4. Number of design variables as a function of column load distribution at basement level



Axial load (DL+0.3LL) under columns at basement level (KN)

Number of variables (Max Load -Min Load)		
≤ 100	≤ 200	≤ 300
3	3	2
[1000,1100]	[1000,1100,1200]	[1000,1100,1200,1300]
[1200,1300]	[1300,1500]	[1500,1600]
[1500,1600]	[1600]	

* $C = H_{eq} \cdot \sqrt{2K_{eff}M}$; $M = W/g$

The design of base isolation was performed by obtaining (or checking) K_{eff} and H_{eq} that give convergent solutions between S_a in Equations 4 and 5 (Figure 4).

2.2. Optimization of Seismic Isolators Layout

Aiming to avoid structural and non-structural damage to the building including isolated layer, and maintain occupant safety during earthquake events, the objective functions used in this step are focused on minimizing the peak roof acceleration (PRA), the inter-story drift ratio (IDR), the bearing displacement (u_b) and maximizing the fundamental period of isolated structure, all without exceeding the limit values recommended by the seismic codes or previous studies. Therefore, the multi-objective optimization problem is formulated as follows:

$$\text{Minimize } \begin{cases} \text{Function1}(X) = \frac{1}{3} \cdot \left(\frac{\text{PRA}}{\text{PRA}_{lim}} + \frac{\text{Max}(\text{IDR}_{story})}{\text{IDR}_{lim}} + \frac{U_{b,max}}{U_{b,lim}} \right) \\ \text{Function2}(X) = \frac{1}{T_{eff}} \end{cases} \quad (8)$$

$$\text{Subject to: } \begin{cases} \text{PRA} \leq \text{PRA}_{lim} \\ \text{Max}(\text{IDR}_{max,story}) \leq \text{IDR}_{lim} \\ u_{b,max} \leq u_{b,lim} \end{cases} \quad (9)$$

where PRA_{lim} is the limit value of peak roof acceleration, $\text{Max}(\text{IDR}_{max,story})$ is the maximum value of the inter-story drift ratio of the superstructure, IDR_{lim} is the limit value of inter-story drift ratio of the superstructure, u_b is the bearing displacement, $u_{b,lim}$ is the limit value of the bearing displacement, and T_{eff} is the fundamental period of isolated structure. According to Pan et al. [39], the peak roof acceleration is limited to 3 m/s^2 to prevent extended damage to building contents, the inter-story drift ratio should be less than $1/150$ and the bearing displacement should not exceed $\max(0.55D, 3T_r)$ [40] (p. 140), where D is the effective diameter of the rubber bearing; and T_r is the total thickness of the rubber layer. For the selected isolation devices, the minimum diameter of the rubber bearing is 600 mm, and the total rubber thickness is 200 mm. Therefore, the displacement limit for our study is set to 330 mm.

Based on the initial population obtained at the first step, an NSGA-II was employed with parameters configured by Table 5, based on the Python MOO framework (Pymoo), to find the optimal layout of isolation bearings using Fast Nonlinear Analysis (FNA) performed on ETABS V21 software. The ETABS OAPI and Comtypes modules are used to establish an interaction between Python and ETABS. Natural rubber bearings are represented by the "Linear" option of the link/support properties; lead rubber bearings by the "Rubber Isolator" option, which describes bilinear behavior; and high-damping rubber bearings by the "Plastic (Wen)" option, based on the traditional Bouc-Wen model.

Table 5. Genetic algorithm parameters

Population	100
No of Offsprings	40
No of Generations	20
Crossover	Simulated Binary Crossover (SBX)
Mutation	Polynomial Mutation (PM)

3. Case Study

3.1. Models' Description

Two 8-story structures, comprising regular and irregular Category III reinforced concrete 3D frames, built on Class C soil in accordance with ASCE/SEI 7-16 [41], are considered in this study. All floors have a height of 3.2 meters and a 1.5-meter height for the base isolation layer (Figure 5). The strengths of concrete and steel are 25 MPa and 500 MPa respectively. Table 6 provides the geometric characteristics of the two building models, while Figure 7 displays the plan and 3D views used for the analysis in this study. Beams and columns are modeled using frame elements, while floors are modeled as a rigid diaphragm. The building is subjected to a dead load (DL) of 2 kN/m^2 , excluding the self-weight of the elements (slabs, beams, and columns), and a live load (LL) of 3 kN/m^2 . Both of which remain identical on all floors.

For base-isolated models, rubber-bearing isolators are modeled using a link element which acts as a connector to link structural elements to isolators or other non-linear components. This allows the software to accurately simulate the behavior of a rubber bearing under various load conditions. The isolator properties (stiffness, damping ratio, etc.) obtained from the supplier's data are assigned to this connecting element. The models of isolated structures, forming the individuals of the population were created automatically using a Python script by replacing the fixed supports in the

fixed-base structures with the link elements (Figure 6). In addition, a 1.5-meter-high layer of isolation under the ground floor was incorporated. The fast-nonlinear analysis (FNA) method, which is effective for isolated structural systems, is used in nonlinear time history analyses. All non-linearity is restricted to the isolators, while the superstructure is considered to be elastic.

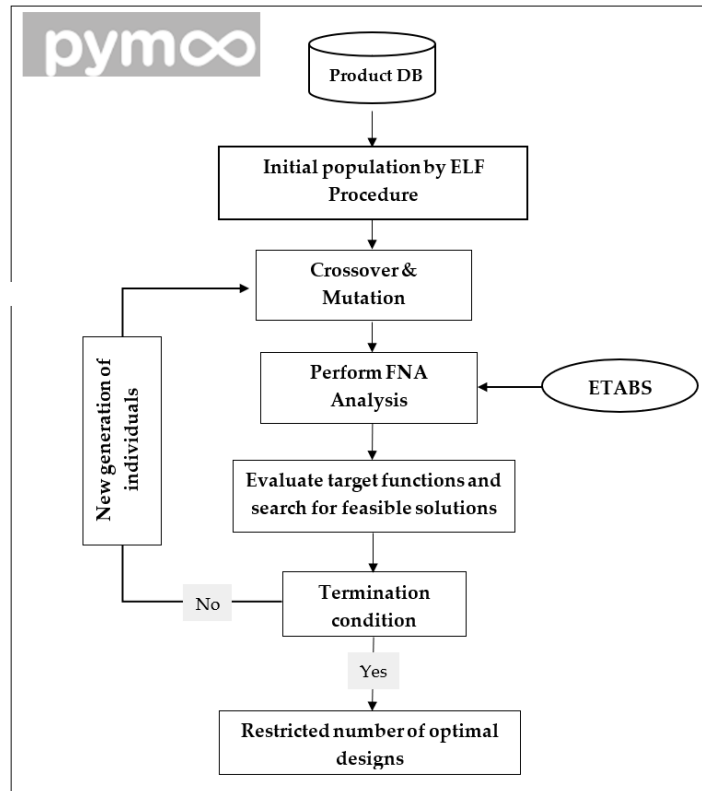


Figure 5. Flow chart of the optimization process

Table 6. The dimensions of frame and slab elements

Model	Dimensions		
	Story 1 --- Story 3	Story 4 --- Story 6	Story 7 --- Story 8
Slab (mm)	200		
Beam Elements (mm × mm)	300×600		
Column Elements (mm × mm)	C1	300×300	300×300
	C2	400×400	300×300
	C3	500×500	400×400

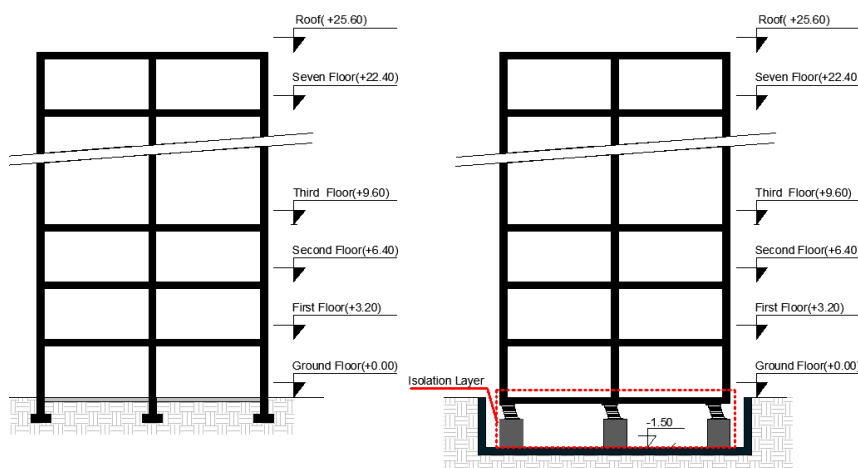


Figure 6. Elevation views: Fixed vs. isolated structure

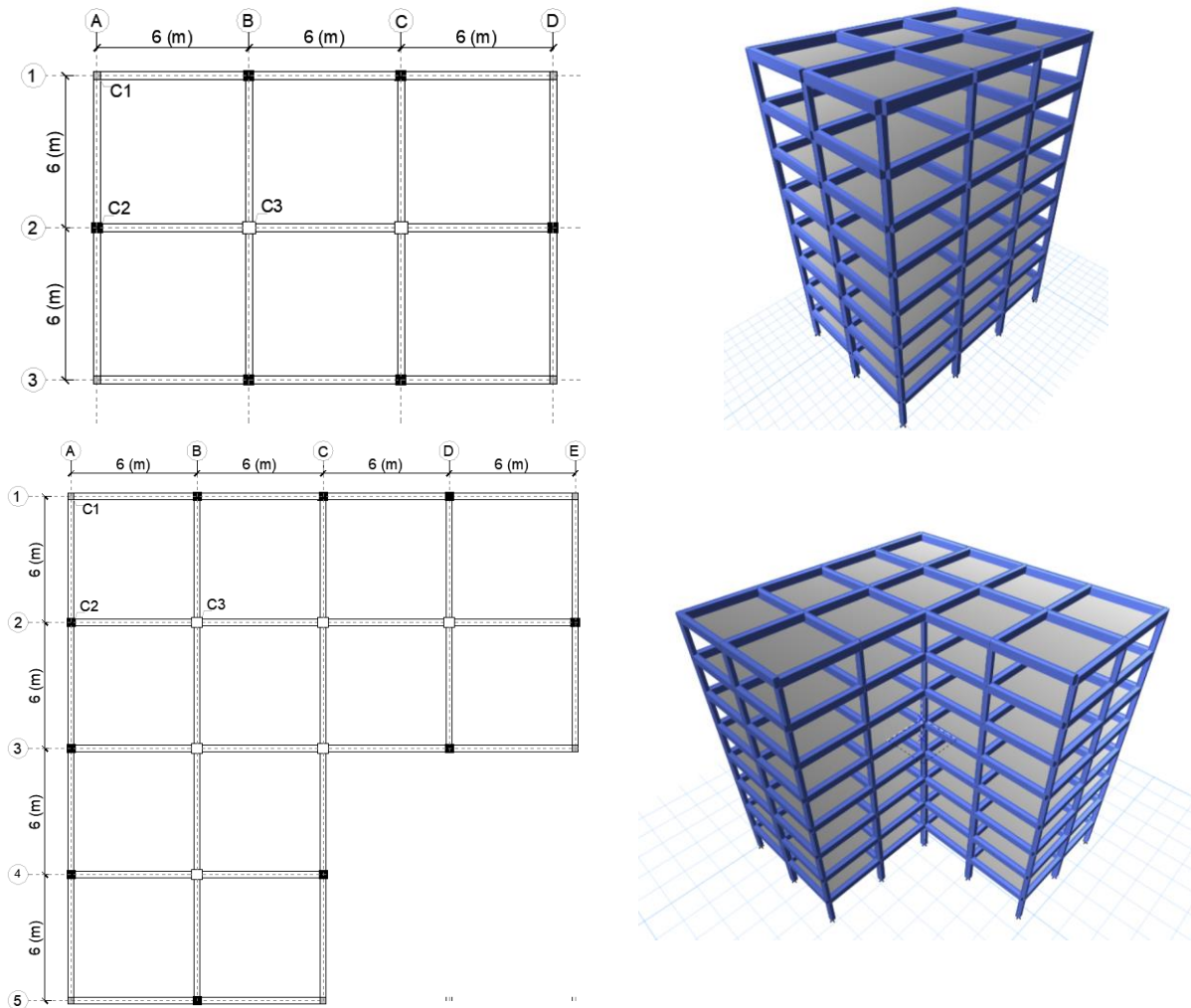


Figure 7. Models views: Plans and 3D views of regular and irregular models used in this study

3.2. Ground Motions Selection

The building is designed to be Category III, built on very dense soil (Class C) in accordance with the ASCE/SEI7-16 code, and it is assumed to be located in San Francisco with a latitude of 37.77712, a longitude of -122.41966 and an elevation of 60.1116 m. The seven design ground motion records were selected from the PEER ground motion database based on the following criteria:

- Magnitudes range from 6.5 to 7.5
- Strike slip type
- $360 \text{ m/s} < V_{s30} < 750 \text{ m/s}$

These records were then scaled using SeismoMatch2023 software, to obtain equivalence and similarity between their response spectra and the design-based earthquake response (DBE) spectrum defined as the target obtained from *ASCE 7 Hazard Tool* [42] (see Figure 8). Table 7 lists the information on the selected natural records with their response sequence numbers. The seismic responses of the structure are analyzed under the seven recordings by applying the fast nonlinear analysis (FNA) method and the values of the desired objective functions (maximum roof acceleration, drift ratio between floors, etc.) are taken equally to the maximum between the averages of the seismic responses under the mentioned recordings in both X and Y directions.

$$SR = \text{Max} \left(\frac{\sum_{\text{records}} SR_X}{N}, \frac{\sum_{\text{records}} SR_Y}{N} \right) \quad (10)$$

where SR is seismic response (Peak roof acceleration, inter story drift ratio), N is number of seismic records ($N=7$).

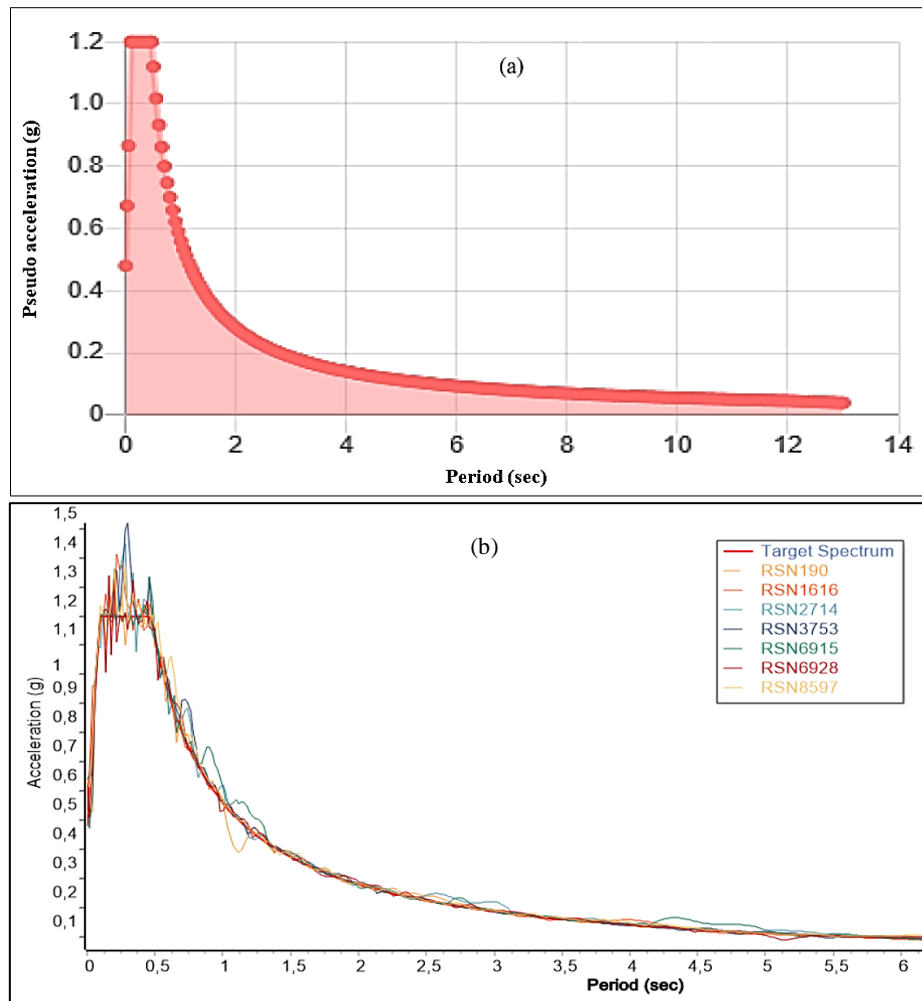


Figure 8. (a) Target spectra of response acceleration for RP = 475 (DBE) - (b) Response spectra of selected seismic waves

Table 7. Informations of recorded earthquakes

RSN	Year	Earthquake name	Magnitude	Epicentral distance (km)	V_{s30} (m/s)
1616	1999	Duzce, Turkey	7.14	23.41	517.0
190	1979	Imperial Valley-06	6.53	24.61	362.38
2714	1999	Chi-Chi-Taiwan-04	6.20	38.11	422.15
3753	1992	Landers	7.28	25.02	422.15
6915	2010	Darfield, New Zealand	7.0	24.36	422.0
6928	2010	Darfield, New Zealand	7.0	25.21	649.67
8597	2010	ELMayor-Cucapah, Mexico	7.2	31.79	503.0

4. Results and Discussion

This study aims to optimize the layout of isolators for seismically isolated base structures based directly on the catalogs of seismic isolator suppliers. The main objectives are as follows:

- Use the ETABS V21 and SeismoMatch V23 programs to model and analyze the models under consideration.
- Apply the NSGA-II genetic algorithm via the Pymoo framework to determine optimal solutions.
- Select the most commonly used seismic isolators from supplier catalogs, including LRB, HDRB, and NRB.
- Use a restricted number of isolators and position them to reduce the eccentricity of the isolation layer.

Three layout models, as illustrated in Figure 9, have been proposed:

- **RN3:** Layout with 3 design variables (3 types of isolators) for the regular structure.

- **IRRN4**: Layout with 4 design variables for the irregular structure.
- **IRRN6**: Layout with 6 design variables for the irregular structure.

We note that the number of design variables (type of isolators) is calculated by placing the same isolator under columns with similar or close loads.

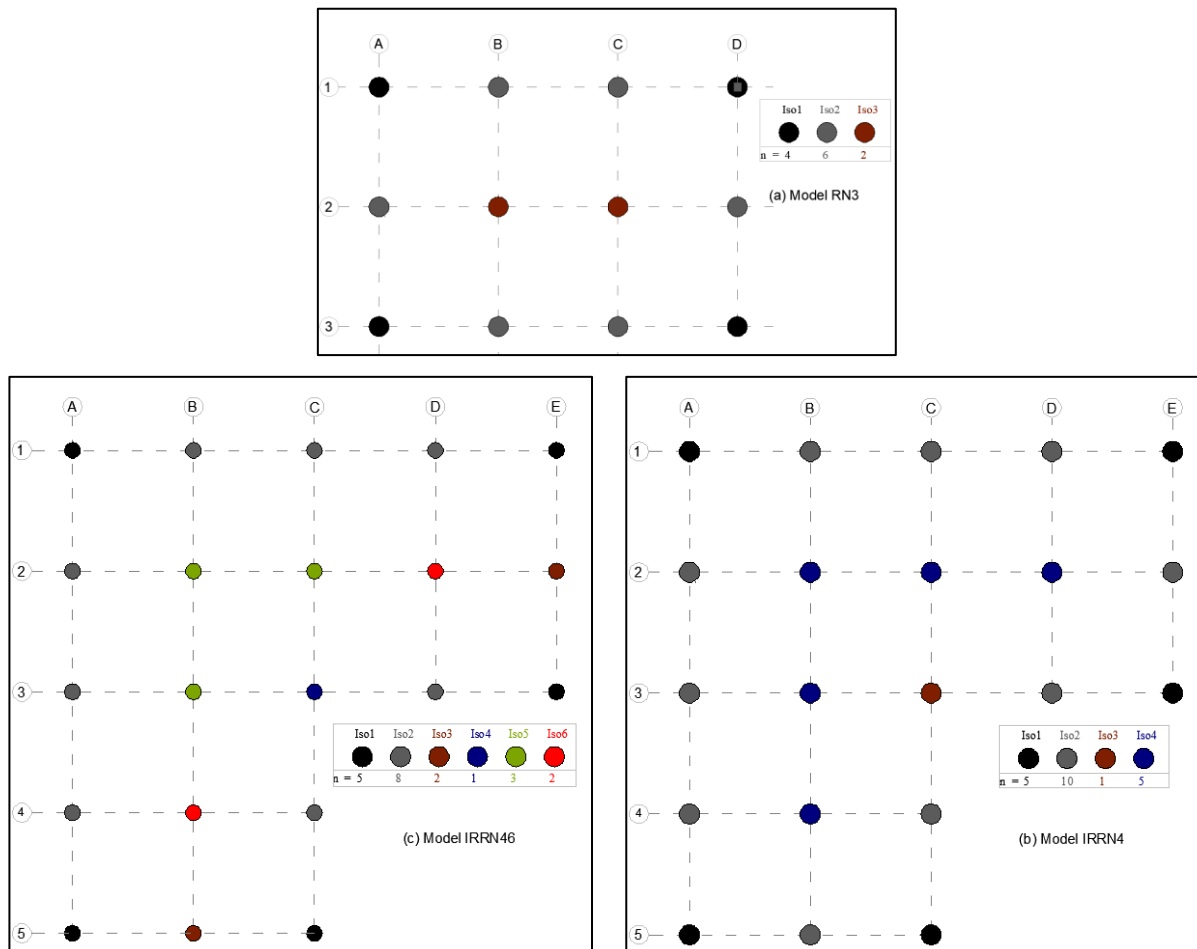


Figure 9. Base isolation layout for used models: (a) RN3, (b) IRRN4, and (c) IRRN6

4.1. Optimal Solutions

The optimal feasible solutions for all models are shown in Table 8. They correspond to a combination of the three isolator types selected from the suppliers' catalogs, and are distributed as follows:

- Seven solutions for the RN3 model;
- One solution for IRRN4;
- Seven solutions for IRRN6.

For all optimal configurations, a symmetrical distribution of isolators is achieved. This result derives from the optimization process in which we forced the placement of the same isolators under columns transmitting identical or similar loads, thus minimizing the eccentricity of the isolation layer and avoiding unfavorable torsional effects that could affect the superstructure. The values of the objective functions considered in the present study for these optimized solutions are shown in Figure 10.

It is important to check the efficiency of the algorithm's convergence throughout the optimization process. Indeed, a stabilization of the process is observed from the 100th iteration for models RN3 and IRRN6, and from the 150th iteration for the IRRN4 model as shown in Figure 11-a. In addition, the evaluation of the hypervolume, (Figure 11-b) with a reference point, was carried out as a measure of the algorithm's performance. According to Blank & Deb [37], a higher hypervolume corresponds to a better set of results confirming the results presented in the previous figure.

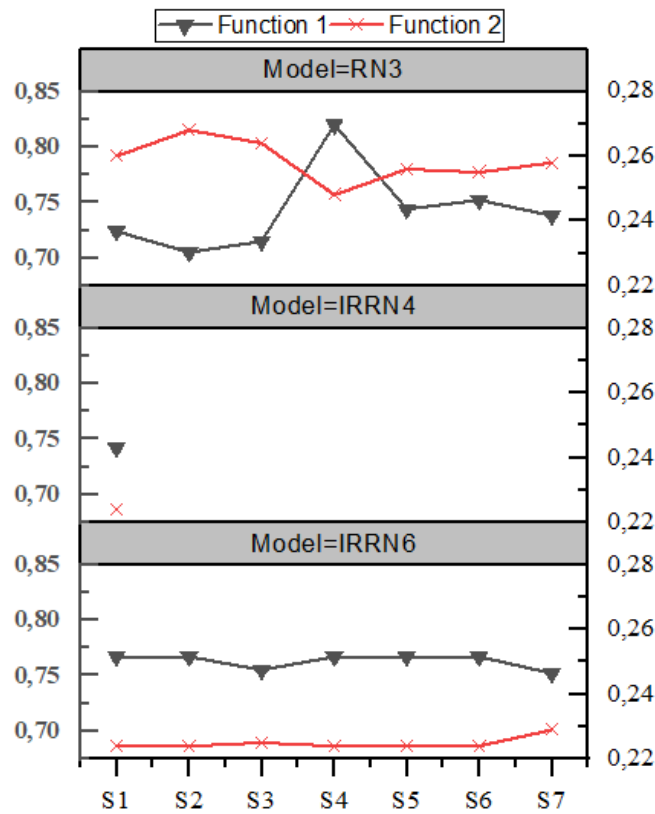


Figure 10. Objective functions for optimal solutions

Table 8. Set of optimal solutions obtained for the models under consideration

Model-IRRN6						
Isolators	ISOL 1	ISOL 2	ISOL 3	ISOL 4	ISOL 5	ISOL 6
Number	5	8	2	1	3	2
S1	NH060G4	LH060G4-11	LH080G4-14	HH060X4S	LH060G4-10	LH060G4-11
S2	NH060G4	LH060G4-11	LH080G4-14	HH060X4S	LH060G4-10	NH060G4
S3	LH060G4-11	LH060G4-10	NH060G4	HH060X4S	NH095G4	NH080G4
S4	NH060G4	LH060G4-11	LH080G4-14	HH060X4S	LH060G4-10	LH080G4-14
S5	NH060G4	LH060G4-11	LH080G4-14	HH060X4S	NH075G4	LH060G4-11
S6	NH060G4	LH060G4-11	LH080G4-14	HH060X4S	NH060G4	NH060G4
S7	LH060G4-10	LH060G4-11	LH060G4-10	HH060X4S	NH070G4	LH075G4-10
Model-IRRN4						
Number	5	10	1	5	-----	-----
S1	HH060X4S	LH060G4-10	HH065X4S	LH060G4-10	-----	-----
Model-RN3						
Number	4	6	2	-----	-----	-----
S1	NH060G4	LH060G4-10	NH060G4	-----	-----	-----
S2	NH060G4	LH060G4-10	LH060G4-10	-----	-----	-----
S3	NH060G4	LH060G4-11	NH060G4	-----	-----	-----
S4	LH060G4-11	NH060G4	NH060G4	-----	-----	-----
S5	LH060G4-11	NH060G4	NH060G4	-----	-----	-----
S6	LH060G4-10	NH060G4	LH060G4-10	-----	-----	-----

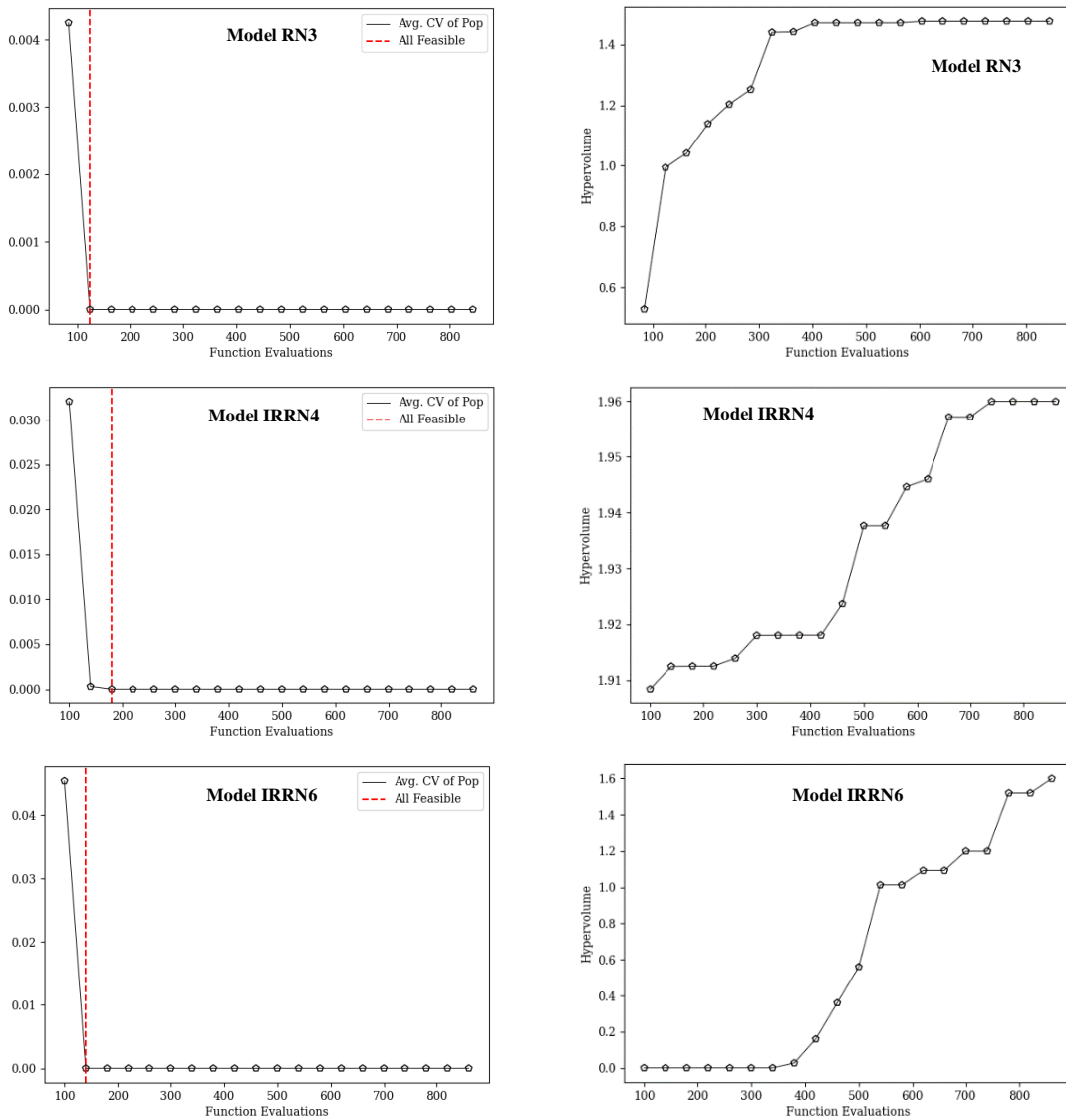


Figure 11. Algorithm Convergence: Average of constraints violation (a) Hypervolume (b)

4.2. Decision Making

The present study has resulted in a set of feasible optimum solutions, taking into account objective functions, constraints, and the number of design variables. The designer is often faced with choosing one solution from several alternatives based on criteria such as structural weight, cost, structural behavior or strength, as well as carbon footprint, etc. In this study, two criteria were taken into account when selecting the final solution: a high fundamental period to reduce seismic forces and associated damages and a reduced weight of the isolation system. The latter being directly associated with the cost of seismic isolation. Figure 12 highlights the selected solutions based on the above-cited criteria: solution 4 for the RN3 model, solution 1 for the IRRN4 model, and solution 6 for the IRRN6 model. The solutions retained for regular and irregular models were analyzed and compared with fixed-base models in the next sections.

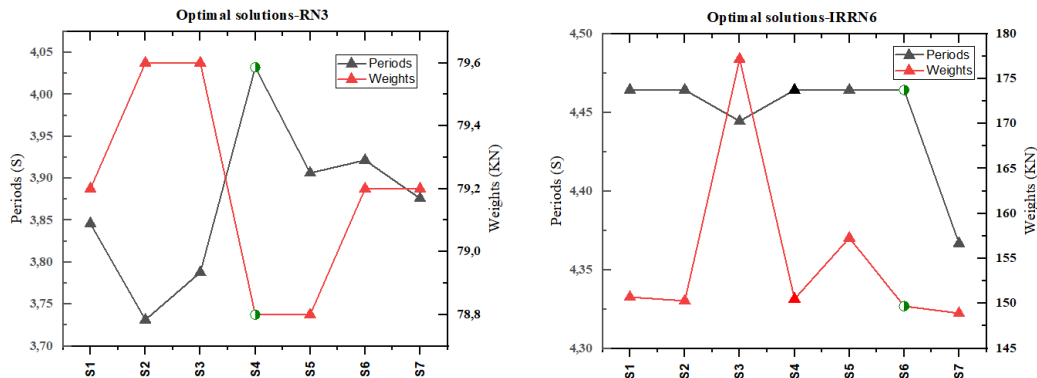


Figure 12. Periods and Devices weights for optimal solutions: RN3 and IRRN6 models

4.3. Fundamental Periods

The fundamental periods of the fixed-base models, as shown in Figure13, are 1.68 s and 2.26 s respectively for regular and irregular structures. In contrast, the selected seismically isolated solutions show fundamental periods of 4.03 s for model RN3 (representing an increase by a factor of 2.4), 4.46 s for model IRRN4, and 4.45 s for model IRRN6 (indicating an increase by a factor of 2). These results are coherent with previous studies where the fundamental periods of seismically isolated structures are generally in the range of 1.5T to 2.5T, where T represents the period of the same fixed-base structure. Almost identical fundamental periods for IRRN4 and IRRN6 models mean that the number of isolator types has no great influence.

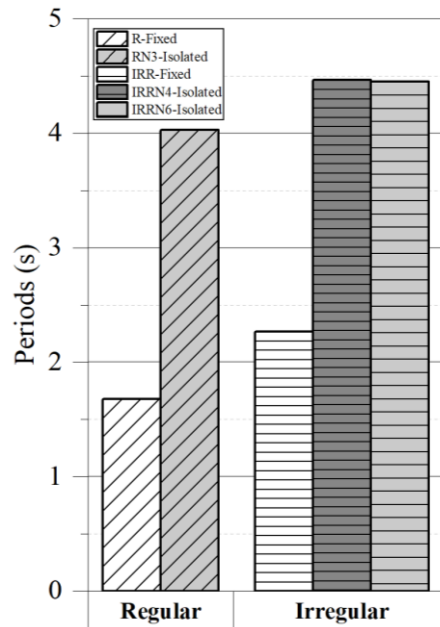


Figure 13. Fundamental Periods Isolated vs Fixed Models

4.4. Base Shear Forces

Switching from a fixed-base model to an isolated structure implies a 56% and 55% reduction in shear forces in both X and Y directions respectively for the regular RN3 model, a 51% reduction in both directions for the irregular IRRN4 model, and a 48% reduction in both directions for the irregular IRRN6 model. Figure 14 shows the extent of the reduction in shear forces for the selected solutions.

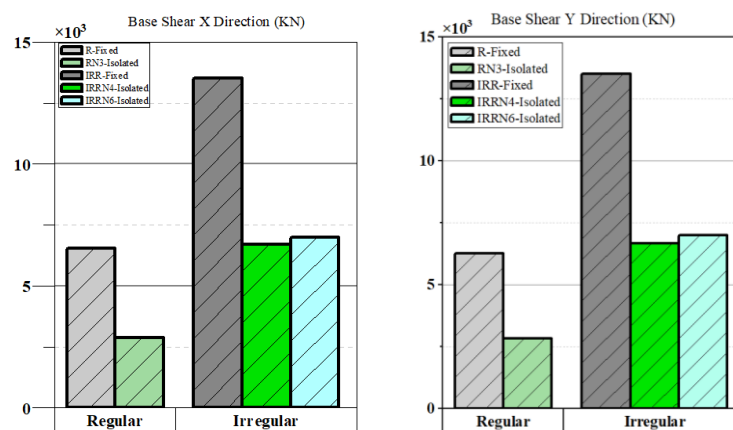


Figure 14. Average base shear force in X and Y directions Isolated vs Fixed models

4.5. Stories Accelerations

The acceleration represents the shock felt during an earthquake. Figure 15 compares the average acceleration in X and Y directions of the stories of the fixed-base and isolated models. It is important to note that the acceleration of isolated structures is significantly lower than that of fixed-base structures, explained by the effectiveness of seismic isolation in reducing the seismic forces transmitted to the superstructure.

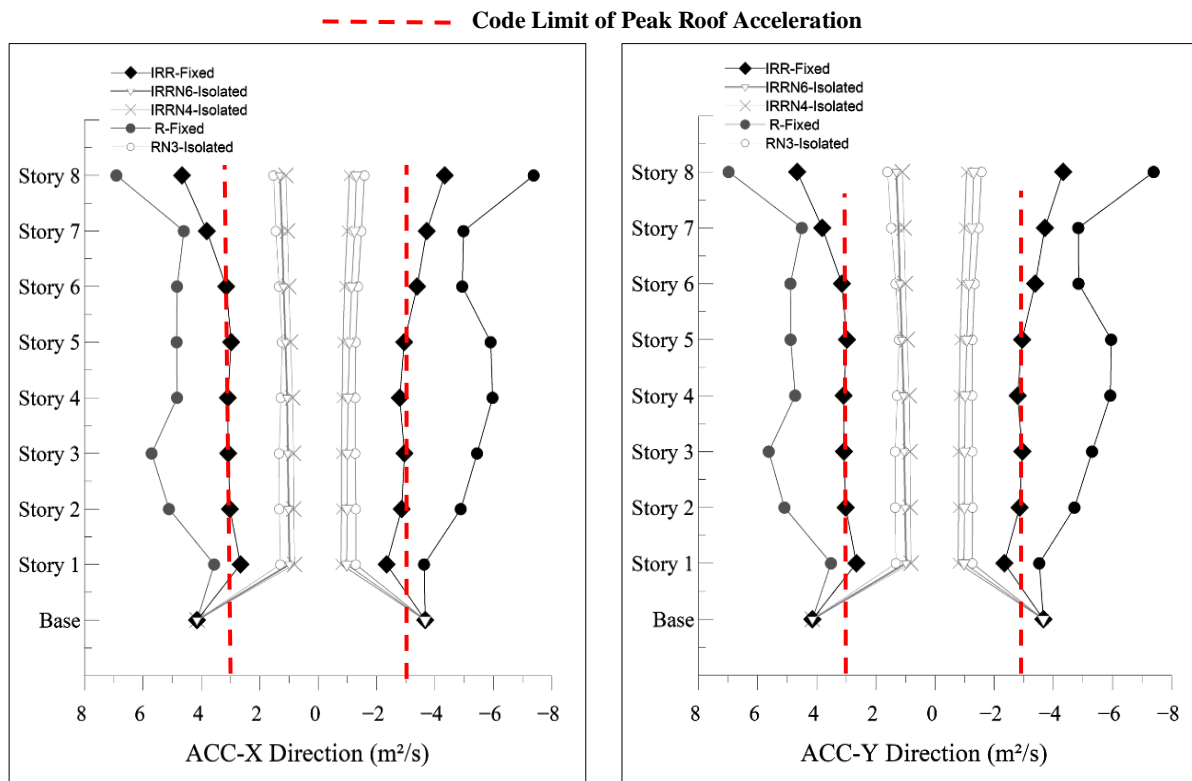


Figure 15. Stories acceleration in X and Y directions fixed vs isolated models

For the fixed-base regular structure, the peak roof acceleration recorded in the Y direction is 6.98 m²/s, while its seismically isolated counterpart reaches 1.61 m²/s, representing a reduction of 77 percent. For the irregular structure, the maximum acceleration at the roof, at around 4.66 m²/s, is the same in both directions. For the seismically isolated structure with 4 types of isolators (IRRN4), the peak roof acceleration is around 1.108 m²/s, representing a 76% reduction. On the other hand, for the structure with 6 types of isolators (IRRN6), the peak roof acceleration is around 1.31 m²/s, resulting in a 72% reduction. In all the cases studied, a significant reduction in acceleration was observed, exceeding 70 percent. This enhances occupant safety, preserves structural contents, and limits seismic damages. In a study published by Belbachir et al. [43], there was a reduction in the acceleration of up to 54% in a reinforced concrete structure with an isolation system consisting of HDRB+FVD. Also, the optimum irregular models with 4 and 6 isolator types (IRRN4 and IRRN6) show almost identical seismic responses, with a marked preference for the IRRN4 model.

5. Conclusions

In order to improve the seismic response of seismically isolated structures, we have proposed an alternative two-stage optimization approach based on the Pymoo framework for optimizing the isolation layer layout. This method aims to overcome the shortcomings of conventional configurations, which are often limited to predefined sizes and a fixed distribution of isolation devices, based on experience or test results, as well as current optimization approaches that focus on isolation layer parameters and require subsequent steps in the selection and choice of isolation devices that can influence the overall performance of the structure. This approach involved first generating an initial population from the supplier catalog that meets buckling and shear stability criteria using the Equivalent Lateral Force (ELF) procedure. Subsequently, optimal solutions were obtained through the application of the NSGA-II genetic algorithm. The specific findings are outlined below:

- For each model considered, a set of optimal layouts has been identified. This allows the designer to choose the configuration best suited to the project context.
- Significant reductions in peak roof acceleration, over 70% compared to fixed base models, which improves the safety of occupants and minimizes structure damage.
- A reduction in base shear force of more than 50% and an increase in the fundamental period by a factor of more than two were observed compared to fixed models.

Based on the results obtained, this study proposes some perspectives and research paths:

- The generalization of the approach to hybrid models with friction and/or elastomer-based isolators and dampers.
- Application of the approach to concrete buildings braced by walls, steel structures, and other types of structures, such as tanks and bridges.

In conclusion, the authors hope that the approach adopted in the present work will help improve the seismic response of seismically isolated buildings while reducing the cost of the isolation layer.

6. Declarations

6.1. Author Contributions

Conceptualization, A.E. and T.T.; methodology, A.E.; software, A.E.; validation, T.T.; formal analysis, A.E.; investigation, A.E.; resources, A.E.; data curation, A.E.; writing—original draft preparation, A.E.; writing—review and editing, T.T.; visualization, A.E.; supervision, T.T. All authors have read and agreed to the published version of the manuscript.

6.2. Data Availability Statement

The data presented in this study are available on request from the corresponding author.

6.3. Funding

The authors received no financial support for the research, authorship, and/or publication of this article.

6.4. Conflicts of Interest

The authors declare no conflict of interest.

7. References

- [1] Yenidogan, C. (2021). Earthquake-Resilient Design of Seismically Isolated Buildings: A Review of Technology. *Vibration*, 4(3), 602–647. doi:10.3390/vibration4030035.
- [2] JSSI (2024). The Japan Society of Seismic Isolation, Tokyo, Japan. Available online: <https://en.jssi.or.jp/en/> (accessed on July 2024).
- [3] Warn, G. P., & Ryan, K. L. (2012). A review of seismic isolation for buildings: Historical development and research needs. *Buildings*, 2(3), 300–325. doi:10.3390/buildings2030300.
- [4] Naeim, F., & Kelly, J. M. (1999). *Design of Seismic Isolated Structures*. John Wiley & Sons, Hoboken, United States. doi:10.1002/9780470172742.
- [5] Shiravand, M. R., Ketabdari, H., & Rasouli, M. (2022). Optimum arrangement investigation of LRB and FPS isolators for seismic response control in irregular buildings. *Structures*, 39, 1031–1044. doi:10.1016/j.istruc.2022.03.070.
- [6] Hu, G. J., Ye, K., & Tang, Z. Y. (2023). Design and analysis of LRB base-isolated building structure for multilevel performance targets. *Structures*, 57, 105236. doi:10.1016/j.istruc.2023.105236.
- [7] Bridgestone. (2017). *Seismic Isolation Product Line-Up*. Bridgestone, Tennessee, United States.
- [8] Zhang, Z., Tian, X., & Ge, X. (2021). Dynamic characteristics of the bouc–wen nonlinear isolation system. *Applied Sciences (Switzerland)*, 11(13), 6106. doi:10.3390/app11136106.
- [9] Gallardo, J. A., de la Llera, J. C., Restrepo, J. I., & Chen, M. (2023). A numerical model for non-linear shear behavior of high damping rubber bearings. *Engineering Structures*, 289, 116234. doi:10.1016/j.engstruct.2023.116234.
- [10] Dai, K., Yang, Y., Li, T., Ge, Q., Wang, J., Wang, B., Chen, P., & Huang, Z. (2022). Seismic analysis of a base-isolated reinforced concrete frame using high damping rubber bearings considering hardening characteristics and bidirectional coupling effect. *Structures*, 46, 698–712. doi:10.1016/j.istruc.2022.10.111.
- [11] Zhou, Z., Li, Y., & Hu, X. (2022). Analysis method of isolation layer composed of high damping rubber bearings based on deformation history integral type model. *Engineering Structures*, 252, 113553. doi:10.1016/j.engstruct.2021.113553.
- [12] Hu, X., & Zhou, Z. (2020). Seismic analysis of a reinforced concrete building isolated by high damping rubber bearings using deformation history integral type model. *Structural Design of Tall and Special Buildings*, 29(18), 1811. doi:10.1002/tal.1811.
- [13] Kazeminezhad, E., Kazemi, M. T., & Mirhosseini, S. M. (2020). Modified procedure of lead rubber isolator design used in the reinforced concrete building. *Structures*, 27, 2245–2273. doi:10.1016/j.istruc.2020.07.056.
- [14] Losanno, D., Hadad, H. A., & Serino, G. (2019). Design charts for eurocode-based design of elastomeric seismic isolation systems. *Soil Dynamics and Earthquake Engineering*, 119, 488–498. doi:10.1016/j.soildyn.2017.12.017.
- [15] Ye, K., Xiao, Y., & Hu, L. (2019). A direct displacement-based design procedure for base-isolated building structures with lead rubber bearings (LRBs). *Engineering Structures*, 197, 109402. doi:10.1016/j.engstruct.2019.109402.
- [16] Lopez-Almansa, F., Piscal, C. M., Carrillo, J., Leiva-Maldonado, S. L., & Moscoso, Y. F. M. (2022). Survey on Major Worldwide Regulations on Seismic Base Isolation of Buildings. *Advances in Civil Engineering*, 2022, 1–16. doi:10.1155/2022/6162698.

- [17] Wu, T. C. (2001). Design of base isolation system for buildings. Ph.D. Thesis, Massachusetts Institute of Technology, Cambridge, United States.
- [18] Mayes, R.L., Naeim, F. (2001). Design of Structures with Seismic Isolation. The Seismic Design Handbook, Springer, Boston, United States. doi:10.1007/978-1-4615-1693-4_14.
- [19] Keikha, H., & Amiri, G. G. (2023). Developing a simplified method for analysis and design of isolated structures with the novel quintuple friction pendulum system under bidirectional near-field excitations. *JVC/Journal of Vibration and Control*, 29(1–2), 453–465. doi:10.1177/10775463211048261.
- [20] Pourzeynali, S., & Zarif, M. (2008). Multi-objective optimization of seismically isolated high-rise building structures using genetic algorithms. *Journal of Sound and Vibration*, 311(3–5), 1141–1160. doi:10.1016/j.jsv.2007.10.008.
- [21] Bakhshinezhad, S., & Mohebbi, M. (2020). Multi-objective optimal design of semi-active fluid viscous dampers for nonlinear structures using NSGA-II. *Structures*, 24, 678–689. doi:10.1016/j.istruc.2020.02.004.
- [22] Tspianitis, A., & Tsompanakis, Y. (2021). Optimizing the seismic response of base-isolated liquid storage tanks using swarm intelligence algorithms. *Computers & Structures*, 243, 106407. doi:10.1016/j.compstruc.2020.106407.
- [23] Tspianitis, A., Spachis, A., & Tsompanakis, Y. (2022). Combined Optimization of Friction-Based Isolators in Liquid Storage Tanks. *Applied Sciences (Switzerland)*, 12(19), 9879. doi:10.3390/app12199879.
- [24] Zou, Z., & Yan, Q. (2022). Artificial Intelligence Algorithm-Based Arrangement Optimization of Structural Isolation Bearings. *Applied Sciences (Switzerland)*, 12(24), 12629. doi:10.3390/app122412629.
- [25] Babaei, M., Taghaddosi, N., & Seraji, N. (2023). Optimal Design of MR Dampers Using NSGA-II Algorithm. *Journal of Soft Computing in Civil Engineering*, 7(1), 72–92. doi:10.22115/SCCE.2022.347247.1466.
- [26] Çerçevik, A. E., Avşar, Ö., & Hasançebi, O. (2020). Optimum design of seismic isolation systems using metaheuristic search methods. *Soil Dynamics and Earthquake Engineering*, 131, 106012. doi:10.1016/j.soildyn.2019.106012.
- [27] Pal, S., Hassan, A., & Singh, D. (2019). Optimization of base isolation parameters using genetic algorithm. *Journal of Statistics and Management Systems*, 22(7), 1207–1222. doi:10.1080/09720510.2019.1614338.
- [28] Dang, Y., Zhao, G. X., Tian, H. T., & Li, G. (2021). Two-Stage Optimization Method for the Bearing Layout of Isolated Structure. *Advances in Civil Engineering*, 2021, 1–10. doi:10.1155/2021/4895176.
- [29] Fallah, N., & Zamiri, G. (2013). Multi-objective optimal design of sliding base isolation using genetic algorithm. *Scientia Iranica*, 20(1), 87–96. doi:10.1016/j.scient.2012.11.004.
- [30] Fallah, N., & Honarparast, S. (2013). NSGA-II based multi-objective optimization in design of Pall friction dampers. *Journal of Constructional Steel Research*, 89, 75–85. doi:10.1016/j.jcsr.2013.06.008.
- [31] Song, Z., Zhai, C., Ma, Y., Wang, Z., & Pei, S. (2024). Multi-stage and multi-objective design optimization for improving resilience of base-isolated hospital buildings. *Engineering Structures*, 304, 117644. doi:10.1016/j.engstruct.2024.117644.
- [32] Kandemir, E. C., & Mortazavi, A. (2022). Optimization of Seismic Base Isolation System Using a Fuzzy Reinforced Swarm Intelligence. *Advances in Engineering Software*, 174, 103323. doi:10.1016/j.advengsoft.2022.103323.
- [33] Ocak, A., Nigdeli, S. M., Bekdaş, G., Kim, S., & Geem, Z. W. (2022). Optimization of Seismic Base Isolation System Using Adaptive Harmony Search Algorithm. *Sustainability (Switzerland)*, 14(12), 7456. doi:10.3390/su14127456.
- [34] Taymus, R. B., Aydogdu, I., Carbas, S., & Ormecioglu, T. O. (2024). Seismic design optimization of space steel frame buildings equipped with triple friction pendulum base isolators. *Journal of Building Engineering*, 92, 109748. doi:10.1016/j.jobe.2024.109748.
- [35] Öncü-Davas, S., Temür, R., & Alhan, C. (2022). Comparison of meta-heuristic approaches for the optimization of non-linear base-isolation systems considering the influence of superstructure flexibility. *Engineering Structures*, 263, 114347. doi:10.1016/j.engstruct.2022.114347.
- [36] Ocak, A., Melih Nigdeli, S., & Bekdaş, G. (2023). Optimization of the base isolator systems by considering the soil-structure interaction via metaheuristic algorithms. *Structures*, 56, 104886. doi:10.1016/j.istruc.2023.104886.
- [37] Blank, J., & Deb, K. (2020). Pymoo: Multi-Objective Optimization in Python. *IEEE Access*, 8, 89497–89509. doi:10.1109/ACCESS.2020.2990567.
- [38] Murota, N., Suzuki, S., Mori, T., Wakishima, K., Sadan, B., Tuzun, C., Sutcu, F., & Erdik, M. (2021). Performance of high-damping rubber bearings for seismic isolation of residential buildings in Turkey. *Soil Dynamics and Earthquake Engineering*, 143, 106620. doi:10.1016/j.soildyn.2021.106620.
- [39] Pan, P., Zamfirescu, D., Nakashima, M., Nakayasu, N., & Kashiwa, H. (2005). Base-isolation design practice in japan: Introduction to the post-kobe approach. *Journal of Earthquake Engineering*, 9(1), 147–171. doi:10.1080/13632460509350537.

- [40] GB50011-2010. (2010). Code for seismic design of buildings. Ministry of Housing and Urban-Rural Development of the People's Republic of China, Beijing, China.
- [41] ASCE/SEI 7-16. (2017). Minimum design loads and associated criteria for buildings and other structures. American Society of Civil Engineers (ASCE), Reston, United States.
- [42] ASCE (2024). ASCE Hazard Tool. American Society of Civil Engineers (ASCE), Reston, United States. Available online: <https://gis.asce.org/beta-7-22/> (accessed on July 2024).
- [43] Belbachir, A., Benanane, A., Ouazir, A., Harrat, Z. R., Hadzima-Nyarko, M., Radu, D., Işık, E., Louhibi, Z. S. M., & Amziane, S. (2023). Enhancing the Seismic Response of Residential RC Buildings with an Innovative Base Isolation Technique. *Sustainability (Switzerland)*, 15(15), 11624. doi:10.3390/su151511624.